

Optimal Control with Stochastic Principles for Voltage Decoupling Control of a Wind Turbine

N. Schinas*

Department of Electrical Engineering, Technological Educational Institute of Western Greece, Patras, Greece

*Corresponding author: nickschinas@gmail.com, nschinas@teiwest.gr

Abstract This paper presents new control strategies for a variable speed wind turbine (WT) which consists of a doubly fed asynchronous generator. In this kind of generators, the rotor windings are supplied with an appropriate voltage v_r through a dc link. There are 2 converters: the rotor-side and the grid-side converter in the dc link. The right pulsation of the rotor-side converter defines the rotor voltage v_r in such a way that both real power maximization from the wind speed and nominal voltage are secured at the same time. With all the flux dynamics inside the machine having been included in the generator model, there is a 2-input-2-output system. Based on the dq electric machines analysis theory, the proposed control scheme manages to create 2 single-input-single-output systems with the rotor voltage component in each axis responsible only for real power or voltage nominal value respectively. This is achieved through optimal control theory with the right definition of the cost function. A new control scheme that contains stochastic control principles is proposed for the grid-side controller in which the decoupling of the loops is achieved by means of the grid frequency being regarded as a 'random' variable to the voltage control loop and so it has no impact on it. The nonlinear system has been tested in the SIMULINK software under 3 tests: In the first test the wind speed changes and brings about an analogous alteration of the WT output. In the second test there is a short circuit in the grid. According to the new rules, the WT is not disconnected from the grid during the short circuit and continues to produce energy with a very smooth behavior. In the third test, there is a large load disturbance in the grid. Again the WT manages to supply the grid with electrical energy in a nice way. Under all tests the controllers seem to cooperate very well and the variations of the voltage and the frequency are within acceptable limits.

Keywords: wind turbine, asynchronous motor, doubly fed induction generator, optimal control

Cite This Article: N. Schinas, "Optimal Control with Stochastic Principles for Voltage Decoupling Control of a Wind Turbine." *American Journal of Electrical and Electronic Engineering*, vol. 5, no. 2 (2017): 40-47. doi: 10.12691/ajeec-5-2-2.

1. Introduction

There have been many proposals about the control schemes for both the rotor side and the grid side converter of a doubly fed wind turbine using induction generator (DFIG) but most of them intend to make the WT work satisfactorily in steady state conditions capturing maximum power from the wind. The increased need for wind energy development makes the installation of WTs in 'weak' ac grids necessary. Besides, a number of voltage instability incidents have been experienced around the world and so, voltage stability has become a major research area in the field of power systems [1,2]. In order voltage stability to be secured, the grid codes in some countries demand that the WT remains connected to the grid for voltage levels as low as 15% of the nominal voltage for 625 ms [3,4,10].

The control design techniques presented in this paper are based on the theory of the dq analysis of the asynchronous generator and the Direct Current (DC) link in the rotor and intend to make the WT have a smooth performance under steady and transient state when it is connected to a very

weak system. Besides, the performance of the designed controllers ensure stability of the system under large voltage sags in order the above grid demands to be met.

The dq model demands two inputs: the voltage v_q in the q-axis and the voltage v_d in the d-axis respectively. There are actually two outputs (y) of the model: the mechanical speed of the rotor of the generator which determines the real power output of the machine and the stator voltage which is relevant to the reactive power of the WT. If we do not neglect the flux dynamics in each axis, the dq theory based on all the machine equations results in equations of the form $y = G_a(s)v_q + G_b(s)v_d$ in the s-plane for every output. We actually have a 2-input-2-output system and this is depicted in Figure 1. As we can see, there is no real mathematical decoupling between the two main loops in the machine with all fluxes transient states being taken into consideration.

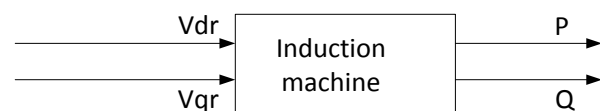


Figure 1. The induction machine as a system with 2 inputs and 2 outputs

In this paper, a completely new way of handling the inputs v_q and v_d is proposed. In the proposed control methods, the input rotor voltage v_{qr} regulates only the stator voltage v_s and so determines only the reactive power of the system. In the same way, the input rotor voltage v_{dr} is responsible for only the real power of the system. Although these refer to the rotor side converter control, a similar method has been developed for the grid side converter control also.

The control methods have been designed based on the linearized models of the systems but the controllers have been tested in the nonlinear system of the WT. The system under study is shown in Figure 2. A wind park (WP) that consists of 3 DFIGs with rated power of 2 MW each, is connected to a weak medium voltage ac grid with short-circuit capacity equal to 150 MVA via a medium voltage line of 20 km. There also is a large asynchronous motor in the grid representing the various inductive loads. We test the system under wind speed changes, short-circuit conditions in the grid and load variations. The recent rules in some grid companies demand that the machine is not disconnected during specific short-circuit conditions but this means that the machine must have a smooth response in this case. The proposed controllers give extremely good performance of the nonlinear system in all transient conditions.

2. Description and Modeling of the System

2.1. Mathematical Model of the Asynchronous Generator

In Figure 3 a general configuration of the WT using an asynchronous generator is depicted. The afore-mentioned

v_{dr} , v_{qr} voltages are the voltages that must be applied to the rotor windings of the generator and this is the scope of the rotor-side converter control scheme.

According to [5,11], the nonlinear reduced-order model of the induction generator based on the theory of the d and q axis, is given by:

$$\begin{aligned} \dot{\lambda}_{qr} &= -R_r i_{qr} - \omega_{slip} \lambda_{dr} + v_{qr}, \\ \dot{\lambda}_{dr} &= -R_r i_{dr} + \omega_{slip} \lambda_{qr} + v_{dr}. \end{aligned}$$

where: $\omega_{slip} = \omega_s - \omega_g$, ω_g is the generator angular speed, ω_s is the synchronous speed, R_r is the rotor resistance, λ_{dr} , λ_{qr} are the d and q components of the rotor magnetic flux respectively, v_{dr} , v_{qr} are the d and q components of the rotor voltage as imposed on it from the rotor side converter.

By substitution of the values given at the Table A1 of the Appendix, we get:

$$\begin{aligned} \dot{\lambda}_{qr} &= -0.0011 i_{qr} - \omega_{slip} \lambda_{dr} + v_{qr}, \\ \dot{\lambda}_{dr} &= -0.0011 i_{dr} + \omega_{slip} \lambda_{qr} + v_{dr}. \end{aligned} \tag{1}$$

The linearization of the above system around an operation point (λ_{qr0} , λ_{dr0} , i_{qr0} , i_{dr0} , ω_{slip0} , v_{dr0} , v_{qr0}) is:

$$\Delta \dot{\lambda}_{qr} = -0.0011 \Delta i_{qr} - \lambda_{dr0} \Delta \omega_{slip} - \omega_{slip0} \Delta \lambda_{dr} + \Delta v_{qr}. \tag{2}$$

$$\Delta \dot{\lambda}_{dr} = -0.0011 \Delta i_{dr} + \lambda_{qr0} \Delta \omega_{slip} + \omega_{slip0} \Delta \lambda_{qr} + \Delta v_{dr}. \tag{3}$$

From the definition of ω_{slip} , it is: $\Delta \omega_{slip} = -\Delta \omega_g$. By substitution of the parameters values given at the Appendix in equations (2)-(3) we get:

$$\Delta \dot{\lambda}_{qr} = -0.0011 \Delta i_{qr} + 31.4 \Delta \lambda_{dr} + 0.4 \Delta \omega_g + \Delta v_{qr} \tag{4}$$

$$\Delta \dot{\lambda}_{dr} = -0.0011 \Delta i_{dr} - 31.4 \Delta \lambda_{qr} + 1.86 \Delta \omega_g + \Delta v_{dr} \tag{5}$$

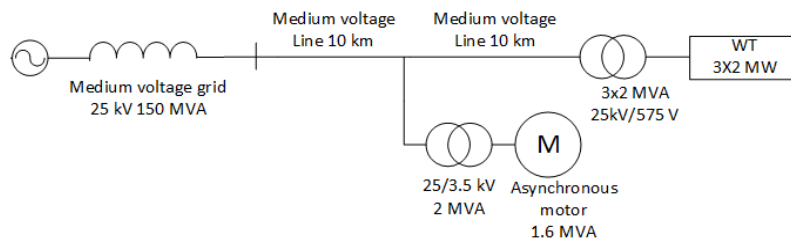


Figure 2. System under study

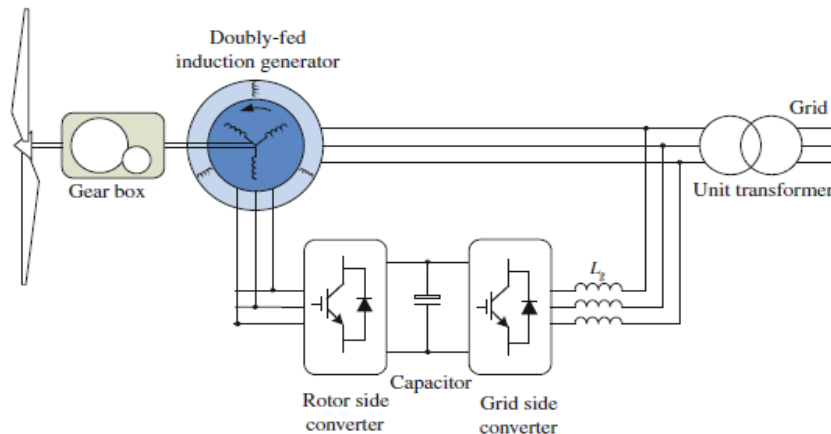


Figure 3. General configuration of the DFIG

From the general theory of the machine we also have [5]:

$$\begin{aligned}\lambda_{ds} &= L_s i_{ds} + L_M i_{dr}, \lambda_{dr} = L_r i_{dr} + L_M i_{ds}, \\ \lambda_{qs} &= L_s i_{qs} + L_M i_{qr}, \lambda_{qr} = L_r i_{qr} + L_M i_{qs},\end{aligned}$$

from which we get:

$$\begin{aligned}\lambda_{qs} &= \frac{L_s}{L_M} \lambda_{qr} + \frac{L_M^2 - L_s L_r}{L_M} i_{qr}, \\ \lambda_{ds} &= \frac{L_s}{L_M} \lambda_{dr} + \frac{L_M^2 - L_s L_r}{L_M} i_{dr}.\end{aligned}\quad (6)$$

We take into consideration that

$$\begin{aligned}v_{qs} &= R_s i_{qs} + \omega_s \lambda_{ds} \approx \omega_s \lambda_{ds}, \\ v_{ds} &= R_s i_{ds} - \omega_s \lambda_{qs} \approx -\omega_s \lambda_{qs}.\end{aligned}\quad (7)$$

From (6), (7) and substitution we have:

$$v_{qs} = 326.6 \lambda_{dr}, v_{ds} = -326.6 \lambda_{qr}. \quad (8)$$

We get the linearized equation for the stator voltage v_s as:

$$v_s^2 = v_{qs}^2 + v_{ds}^2 \Rightarrow 2v_{s0} \Delta v_s = 2v_{qs0} \Delta v_{qs} + 2v_{ds0} \Delta v_{ds}. \quad (9)$$

From (8), (9) it is:

$$\begin{aligned}\Delta v_s &= \frac{v_{qs0}}{v_{s0}} \Delta v_{qs} + \frac{v_{ds0}}{v_{s0}} \Delta v_{ds} \\ &= 326.6 \frac{v_{qs0}}{v_{s0}} \Delta \lambda_{dr} - 326.6 \frac{v_{ds0}}{v_{s0}} \Delta \lambda_{qr}.\end{aligned}$$

By substitution of the values from the Appendix we have:

$$\Delta v_s = -326.6 \Delta \lambda_{qr}. \quad (10)$$

2.2. Mathematical Model of the Wind Turbine

The two-mass drive train model for the WT system is used in this paper as the dynamic characteristics of the WT can be reproduced satisfactorily because the low speed axis is relatively soft. The gear box and the high speed axis are assumed to be infinitely stiff. The angular velocity of the rotor ω_t is given by [6]:

$$\dot{\omega}_t = \frac{1}{2H_t} (T_t - NK_s \gamma),$$

where: H_t is the low speed inertia constant, T_t is the aerodynamic torque from the wind speed, N is the gear ratio, K_s is the torsion stiffness, γ is the torsion angle. The torsion damping constants have been neglected. By substitution from the parameters given in the Appendix, we have:

$$\dot{\omega}_t = 0.000625T_t - 625\gamma. \quad (11)$$

For MPPT operation of the WT, it is [7]: $T_t = K_{opt} \omega_t^2$,

$$K_{opt} = 0.5\rho\pi \frac{R^5}{\lambda_{opt}^3} C_{pmax}. \text{ By substitution:}$$

$$T_t = 117954\omega_t^2, \text{ so (11) becomes:}$$

$$\dot{\omega}_t = 73.72\omega_t^2 - 625\gamma. \quad (12)$$

By linearization around the operation point ω_{t0} we get:

$$\Delta \dot{\omega}_t = 147.4\omega_{t0}\Delta\omega_t - 625\Delta\gamma \quad (13)$$

and by substitution of the value ω_{t0} :

$$\Delta \dot{\omega}_t = 347.12\Delta\omega_t - 625\Delta\gamma. \quad (14)$$

The torsion angle is given by [6]: $\dot{\gamma} = 2\pi f \left(\omega_t - \frac{1}{N} \omega_g \right)$, where ω_g is the rotor angular speed of the induction generator. By substitution:

$$\dot{\gamma} = 314\omega_t - 3.925\omega_g. \quad (15)$$

The slip frequency s of the generator is given by [6]:

$$\dot{s} = \frac{-1}{2H_g \omega_s} (K_s \gamma - T_e), \text{ where } T_e \text{ is the electromechanical}$$

torque of the generator. By substitution we have:

$$\dot{s} = -0.22\gamma + 1.77 * 10^{-5} T_e. \quad (16)$$

The linearized forms of the equations (15)-(16) are:

$$\Delta \dot{\gamma} = 314\Delta\omega_t - 3.925\Delta\omega_g, \quad (17)$$

$$\Delta \dot{s} = -0.22\Delta\gamma + 1.77 * 10^{-5} \Delta T_e.$$

The electromechanical torque is equal to [5]:

$$T_e = \frac{3}{2} p (\lambda_{qr} i_{dr} - \lambda_{dr} i_{qr}). \text{ By linearization we get:}$$

$$\Delta T_e = \frac{3p}{4} \begin{pmatrix} \lambda_{qr0} \Delta i_{dr} + i_{dr0} \Delta \lambda_{qr} \\ -\lambda_{dr0} \Delta i_{qr} - i_{qr0} \Delta \lambda_{dr} \end{pmatrix}. \quad (18)$$

By substitution we have:

$$\Delta T_e = 5538\Delta\lambda_{qr} + 1800\Delta\lambda_{dr} - 1.2\Delta i_{qr} - 5.58\Delta i_{dr}.$$

Also, $\Delta s = -\frac{1}{\omega_s} \Delta \omega_g$. So, the last equation of (17) becomes:

$$\Delta \dot{\omega}_g \approx 69\Delta\gamma - 31\Delta\lambda_{qr} - 10\Delta\lambda_{dr}. \quad (19)$$

2.3. State Space Form

By setting $x = [\Delta\omega_t \ \Delta\gamma \ \Delta\omega_g \ \Delta\lambda_{qr} \ \Delta\lambda_{dr}]^T$ $u = [\Delta v_{qr} \ \Delta v_{dr}]^T$, the above equations (4),(5),(14),(17),(19) are written in state space form $\dot{x} = Ax + Bu + Gw$, where:

$$A = \begin{bmatrix} 347.12 & -625 & 0 & 0 & 0 \\ 314 & 0 & -3.925 & 0 & 0 \\ 0 & 69 & 0 & -31 & -10 \\ 0 & 0 & 0.4 & 0 & 31.4 \\ 0 & 0 & 1.86 & -31.4 & 0 \end{bmatrix}, \quad (20)$$

$$B = \begin{bmatrix} 0 & 0 \\ 0 & 0 \\ 0 & 0 \\ 1 & 0 \\ 0 & 1 \end{bmatrix}, G = \begin{bmatrix} 0 & 0 \\ 0 & 0 \\ 0 & 0 \\ -0.0011 & 0 \\ 0 & -0.0011 \end{bmatrix}, w = \begin{bmatrix} \Delta i_{qr} \\ \Delta i_{dr} \end{bmatrix}$$

The output y of the system is firstly considered to be the stator voltage Δv_s concerning the reactive power loop. From (10) it is in state space form: $y=Cx+Du$, where:

$$C = [0 \ 0 \ 0 \ -326.6 \ 0], \quad D = 0. \quad (21)$$

From (20),(21) the output stator voltage Δv_s in transfer function form is given by:

$$\Delta v_s = G_1(s)\Delta v_{qr} + G_2(s)\Delta v_{dr}, \quad (22)$$

where:

$$G_1(s) = 142.67 \frac{s^2 - 0.52s + 18.57}{s^2 - 444.4s - 524.84},$$

$$G_2(s) = -8 \frac{s^2 - 560s + 344.22}{s^2 - 444.4s - 524.84}.$$

The output y of the system is now considered to be the WT rotor speed $\Delta \omega_r$, concerning the real power loop. From (14) it is in state space form: $y=Cx+Du$, with:

$$C = [1 \ 0 \ 0 \ 0 \ 0], \quad D = 0. \quad (23)$$

From (20), (23) the output WT rotor speed $\Delta \omega_r$ in transfer function form is equal to:

$$\Delta \omega_r = G_3(s)\Delta v_{qr} + G_4(s)\Delta v_{dr}, \quad (24)$$

where:

$$G_3(s) = \frac{B_3(s)}{A(s)} = 0.172 \frac{s - 10.13}{s^2 - 444.4s - 524.84},$$

$$G_4(s) = \frac{B_4(s)}{A(s)} = 0.055 \frac{s + 97.2}{s^2 - 444.4s - 524.84}.$$

2.4. Grid - Side Converter Modelling

Figure 5 shows a general schematic configuration of the grid side converter, where e_a, e_b, e_c are the grid phase voltages and v_a, v_b, v_c are the converter phase voltages. According to the dq analysis of the quantities, we have the following equations for the d,q components (i_d, i_q) of the line currents i_a, i_b, i_c [6]:

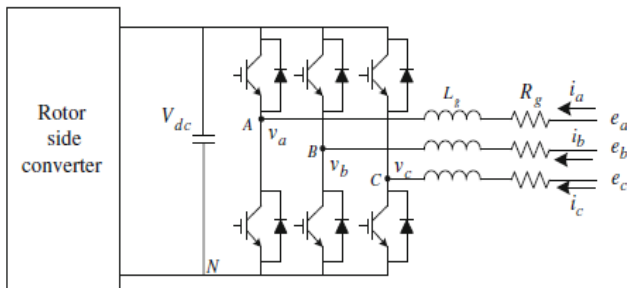


Figure 4. Grid-side configuration of the rotor converter

$$\dot{i}_q = -\frac{R_g}{L_g}i_q - \omega_s i_d - \frac{1}{L_g}v_q, \quad (25)$$

$$\dot{i}_d = -\frac{R_g}{L_g}i_d + \omega_s i_q - \frac{1}{L_g}v_d + \frac{1}{L_g}e_d.$$

The first control loop is the reactive power output regulation through the current i_q . We have assumed for

convenience that the grid voltage e is located on the d-axis. The huge alterations of the WT real power output especially when it works in a weak system may result in alterations of the grid frequency ω_s . For this reason, the parameter ω_s is considered to be a disturbance for the reactive power adjustment loop. The reference $i_{q,ref}$ is achieved through the loop given in the Figure 5a and so the grid voltage e is controlled. The second loop is the real power regulation through the current i_d . The reference $i_{d,ref}$ is achieved through the loop given in the Figure 5b and so the right value of v_{dc} is preserved.

The linearization of (25) around an operation point ($i_{q0}, i_{d0}, v_{q0}, v_{d0}$) results in:

$$\Delta \dot{i}_q = -\frac{R_g}{L_g}\Delta i_q - i_{d0}\Delta \omega_s - \omega_{s0}\Delta i_d - \frac{1}{L_g}\Delta v_q, \quad (26)$$

$$\Delta \dot{i}_d = -\frac{R_g}{L_g}\Delta i_d + i_{q0}\Delta \omega_s + \omega_{s0}\Delta i_q - \frac{1}{L_g}\Delta v_d + \frac{1}{L_g}\Delta e_d.$$

The grid voltage e is constant, so $\Delta e_d = 0$. By substitution of the values from the Appendix into (26) we get:

$$\Delta \dot{i}_q = -0.01\Delta i_q - 314\Delta i_d + 510\Delta \omega_s - 31.25\Delta v_q$$

$$\Delta \dot{i}_q = -0.01\Delta i_d + 314\Delta i_q - 7\Delta \omega_s - 31.25\Delta v_d. \quad (27)$$

In state space form $\dot{x} = Ax + Bu$, with $x = [\Delta i_q \ \Delta i_d]^T$, $u = [\Delta v_q \ \Delta v_d \ \Delta \omega_s]^T$. From (27) the matrices are:

$$A = \begin{bmatrix} -0.01 & -314 \\ 314 & -0.01 \end{bmatrix}, \quad B = \begin{bmatrix} -31.25 & 0 & 510 \\ 0 & -31.25 & -7 \end{bmatrix}. \quad (28)$$

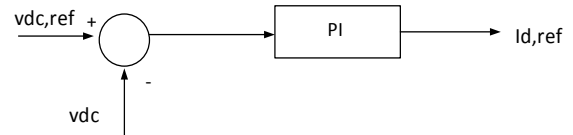


Figure 5a. $I_{d,ref}$ calculation for real power system

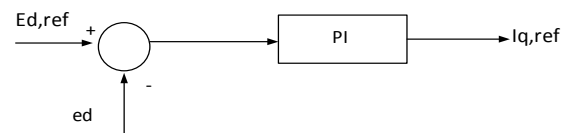


Figure 5b. $I_{q,ref}$ calculation for reactive power system

The reactive power control loop has been designed in this paper. For output $y = \Delta i_q$, we have:

$$C = [1 \ 0], \quad D = 0. \quad (29)$$

From the state space model given by (28), (29) we can have the output Δi_q in transfer function form given by:

$$\Delta i_q = G_5(s)\Delta v_q + G_6(s)\Delta v_d + G_7(s)\Delta \omega_s, \quad (30)$$

where:

$$G_5(s) = \frac{B_5(s)}{A'(s)} = \frac{-31.25s - 0.3125}{s^2 + 98596},$$

$$G_6(s) = \frac{B_6(s)}{A'(s)} = \frac{9812.5}{s^2 + 98596},$$

$$G_7(s) = \frac{C(s)}{A'(s)} = \frac{510s + 2203}{s^2 + 98596}.$$

3. Control Systems Design

3.1. Rotor-side Converter Control

As it has already been developed, the output ω_t (for maximization of real power) and the v_s (for constant stator voltage) depend on the components of the rotor voltage on the dq axis: Δv_{qr} and Δv_{dr} which are regarded as inputs to the system. The objective of the control system in rotor side converter is the construction of two stable decoupled control loops with the voltage component Δv_{qr} to control only Δv_s and the voltage component Δv_{dr} to control only the output $\Delta \omega_t$.

We firstly work on the first loop regarding the reactive power control. We want the output Δv_s to be controlled only by Δv_{qr} . In order this to be achieved we work by means of the optimal control theory.

We set the following quadratic cost function [8,9]:

$$J = \int_0^\infty \left\{ \Delta x^T(t) \Delta u^T(t) \begin{bmatrix} Q(t) & M(t) \\ M^T(t) & R(t) \end{bmatrix} \begin{bmatrix} \Delta x(t) \\ \Delta u(t) \end{bmatrix} \right\} dt.$$

Since we want the output to be controlled only by u_1 , we must minimize the effect of u_2 onto the output. We set the matrices Q, M, R as following:

$$Q = \begin{bmatrix} 0 & 0 & 0 & 0 & 0 \\ 0 & 0 & 0 & 0 & 0 \\ 0 & 0 & 0 & 0 & 0 \\ 0 & 0 & 0 & 1 & 0 \\ 0 & 0 & 0 & 0 & a \end{bmatrix}, M = 0, R = \begin{bmatrix} 1 & 0 \\ 0 & a \end{bmatrix}.$$

The value of a is arbitrary, but it must be high and positive. We set $a = 100000$. The optimal feedback control law is of the form: $\Delta u(t) = C \Delta x(t)$. The value of C was found by means of the MATLAB software and is equal to:

$$C = 10^5 * \begin{bmatrix} 9.061 & -0.775 & -0.11 & 0.0083 & -0.0008 \\ 0 & -0.0001 & 0 & 0 & 0 \end{bmatrix}.$$

The bode diagram for the output from each input is shown in the Figure 7. We can see very clearly that the output actually depends only on the input u_1 . So we ignore the input u_2 and we reach the closed-loop system of Figure 6a by finding the equivalent series controller which is:

$$G_{cl} = \frac{7.8s^2 + 10.7s + 5.1}{-0.155s^2 + 1.312s + 2.6}.$$

If we follow the same procedure for the second loop, we shall come to a similar result regarding the control of $\Delta \omega_t$ only from Δv_{dr} .

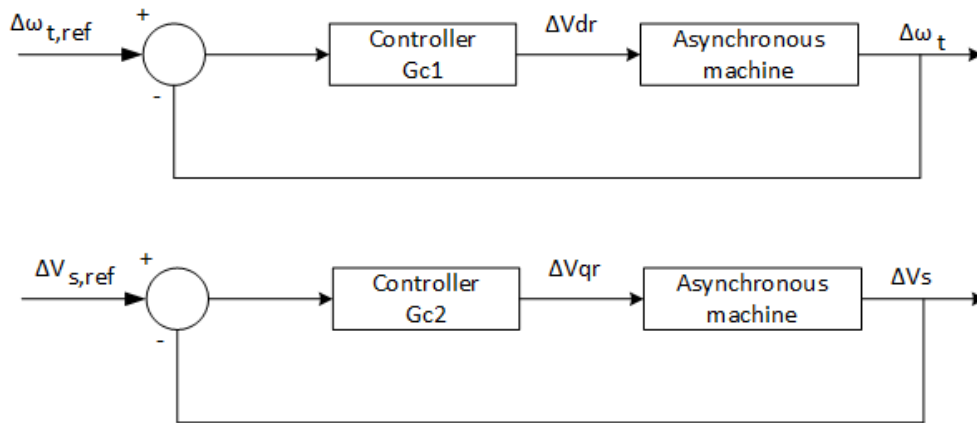


Figure 6. Objective of the control system design

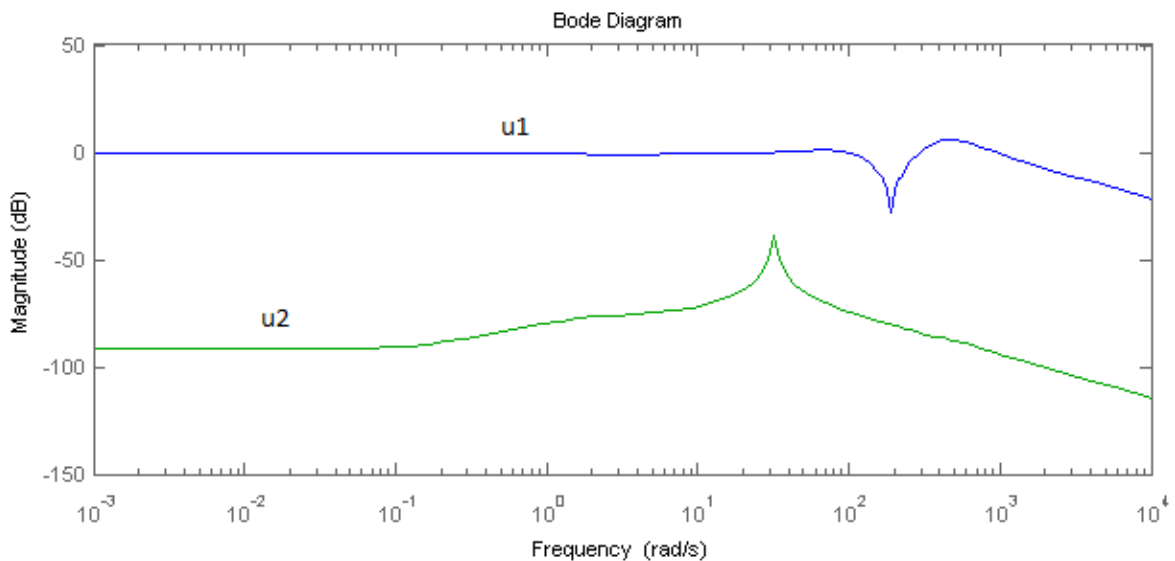


Figure 7. Bode diagrams of the output Δv_s from the 2 inputs

3.2. Grid-side Converter Control

As it seems from (30), the reactive power loop with Δi_q as output y , includes the parameter $\Delta \omega_s$, which actually depends on the change of the active power. The aim of the grid-side converter control is to distinguish the two loops by eliminating the impact of $\Delta \omega_s$ onto Δi_q . In order this to be achieved, we work with the theory of discrete systems. The nonlinear system has been simulated in SIMULINK software with time step size of 200 μ sec. The transfer functions of (30) are converted to z-plane with $T_s = 0.0002$ sec and we get:

$$G_5(z) = \frac{B_5(z)}{A'(z)} = -0.006246 \frac{z-1}{z^2-2z+1},$$

$$G_6(z) = \frac{B_6(z)}{A'(z)} = 0.001962 \frac{z+1}{z^2-2z+1}$$

$$G_7(z) = \frac{C(z)}{A'(z)} = -0.06995 \frac{z-1}{z^2-2z+1}.$$

From (30), if we set $u_1 = \Delta v_q$, $u_2 = \Delta v_d$ and $e = \Delta \omega_s$ it is:

$$y(k) = \frac{B_5(z)}{A'(z)} u_1(k) + \frac{B_6(z)}{A'(z)} u_2(k) + \frac{C(z)}{A'(z)} e(k) \quad (31)$$

$$\Rightarrow y(k) = \frac{B_1^*}{A^*} z^{-d} u_1(k) + \frac{B_2^*}{A^*} z^{-d} u_2(k) + \frac{C^*}{A^*} e(k)$$

where $d = \deg A' - \deg B_1$ (or B_2) and general any function X^* is the reciprocal of X , that is $X^*(z^{-1}) = z^{-n} X(z)$ and z^{-1} is the backward-shift operator in the z plane. It is assumed that X is of order n .

Supposing that C^* and A^* are of the same order, we can write:

$$\frac{C^*}{A^*} = F^* + z^{-d} \frac{G^*}{A^*},$$

then after d situations the output y will be:

$$y(k+d) = \frac{B_1^*}{A^*} u_1(k) + \frac{B_2^*}{A^*} u_2(k) + F^* e(k+d) + \frac{G^*}{A^*} e(k).$$

From (31) it is:

$$e(k) = \frac{A^*}{C^*} y(k) - \frac{B_1^*}{C^*} z^{-d} u_1(k) - \frac{B_2^*}{C^*} z^{-d} u_2(k).$$

By substitution to the previous we have:

$$y(k+d) = F^* e(k+d) + \frac{G^*}{C^*} y(k) \quad (32)$$

$$+ \frac{B_1^* F^*}{C^*} u_1(k) + \frac{B_2^* F^*}{C^*} u_2(k).$$

Now, we must recall that $u_1 = v_d = V \cos \delta$ and $u_2 = v_q = V \sin \delta$ where V is the rated value of phase voltage and δ is the angle between the voltages v_a and e_a , as these voltages are depicted in Figure 4. So the inputs in the linearized model are:

$$v_d^2 + v_q^2 = v^2 \Rightarrow \Delta(v_d^2 + v_q^2) = \Delta v^2$$

$$\Rightarrow 2v_{dg0} \Delta V_d + 2v_{qg0} \Delta V_q = 0$$

$$\Rightarrow v_{dg0} u_1 + v_{qg0} u_2 = 0 \Rightarrow u_1 = -\frac{v_{qg0}}{v_{dg0}} u_2 = m u_2.$$

By substitution to the previous we have:

$$y(k+d) = F^* e(k+d) + \frac{G^*}{C^*} y(k) + \frac{(B_1^* + m B_2^*) F^*}{C^*} u_1(k).$$

The output must converge and this is best accomplished when $Var(y(k+d)) = 0$.

By setting $\frac{(B_1^* + m B_2^*) F^*}{C^*} = x$ we have:

$$Var \left[F^* e(k+d) + \frac{G^*}{C^*} y(k) + x u_1(k) \right]$$

$$= Var \left[F^* e(k+d) \right] + Var \left[\frac{G^*}{C^*} y(k) + x u_1(k) \right]$$

$$+ 2Cov \left[F^* e(k+d), \left(\frac{G^*}{C^*} y(k) + x u_1(k) \right) \right] = 0.$$

The first and the third term are equal to zero because the signal $e(k)$ has zero mean value as it is considered to be an independent random variable and we want it to be irrelevant to the voltage – control loop. So from the previous equation:

$$Var \left[\frac{G^*}{C^*} y(k) + x u_1(k) \right] = 0.$$

The optimal and simpler solution to this demand is:

$$\frac{G^*}{C^*} y(k) + x u_1(k) = 0 \Rightarrow u_1 = -\frac{\frac{G^*}{C^*}}{(B_1^* + m B_2^*)} y(k).$$

This is the control law for input u_1 . From the previous it is:

$$u_2 = \frac{1}{m} u_1. \text{ This is the control law for input } u_2.$$

4. Nonlinear System Simulation Results

The system under study as has been depicted in Figure 1 has been simulated in SIMULINK software. The rated values for the machines are listed in the Appendix. The wind speed has been simulated as a series of random numbers around a mean value. In the first case we consider the wind speed to be altered at $t = 9$ sec (Figure 8) from an average value of 7 m/s to an average value of 12 m/s. The response of the system is shown in Figure 9. The change of the power from the WT follows the change of the wind speed (Figure 9a), the grid voltage is constant (Figure 9b) and the motor speed (which depends on the grid frequency) is also constant (Figure 9c).

In the second case, (Figure 10), at $t = 36$ sec there is a 3-phase short-circuit in the grid for a time duration of 400msec. According to new grid rules, the WT is not disconnected. The WP manages to deliver a small amount of real power into the grid during the short circuit. When

the fault is cleared, the WP starts to produce power again with no serious transient problems and a very smooth behavior. The response of the system is depicted in Figure 10. The grid voltage is in Figure 10a, the WP output is shown in Figure 10b and the motor speed in Figure 10c.

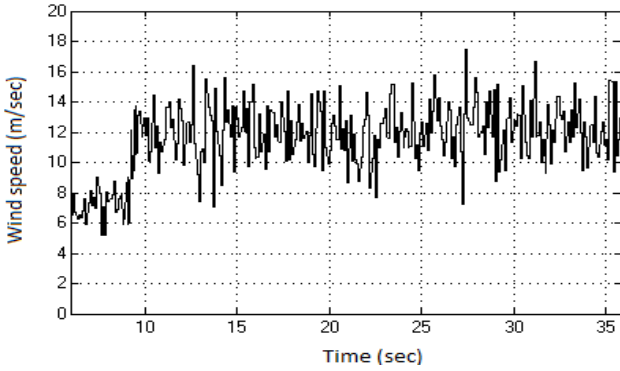


Figure 8. Wind speed for the first test of the system

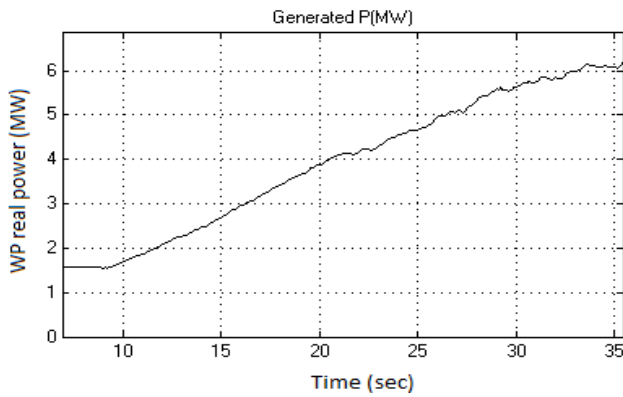


Figure 9a. WT real power output

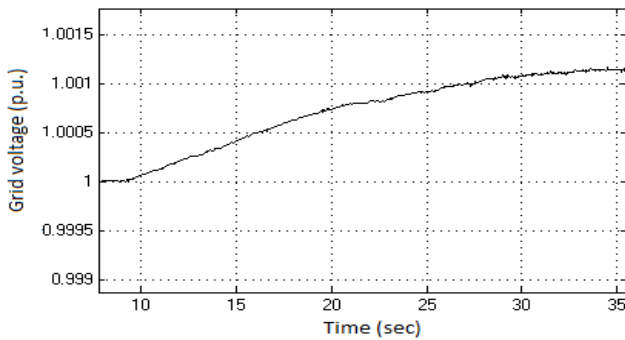


Figure 9b. Grid voltage

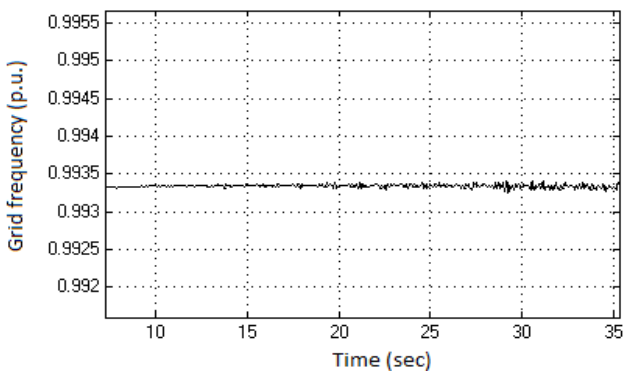


Figure 9c. Grid frequency

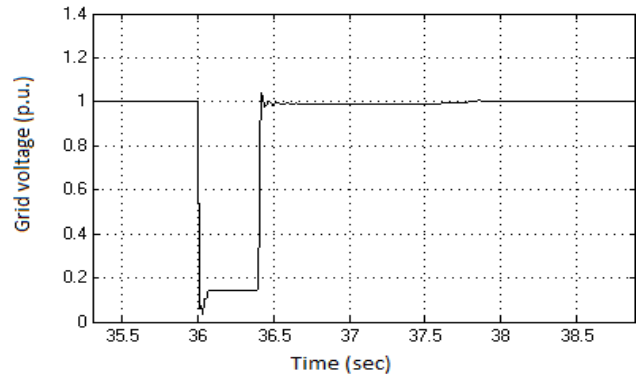


Figure 10a. Grid voltage with the short-circuit

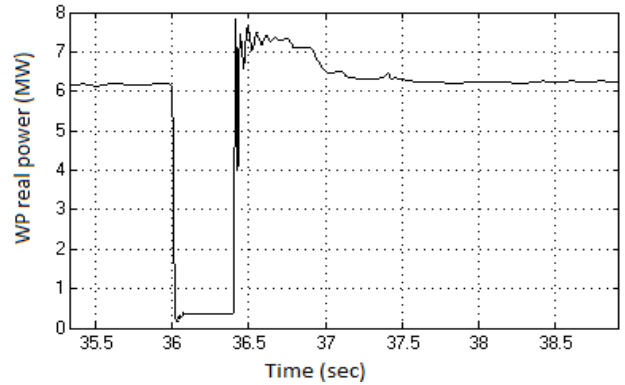


Figure 10b. WP real power during and after a short-circuit

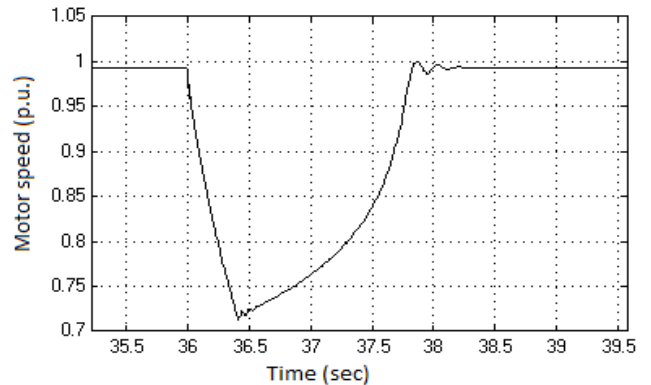


Figure 10c. Motor speed during and after short-circuit

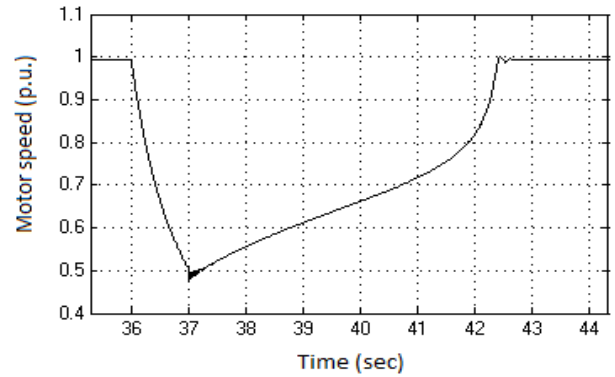


Figure 11a. Motor speed for motor disturbance

In the third test, there is a severe load disturbance near the WP. The motor is disconnected at $t = 36$ sec and reconnected again at $t = 37$ sec. This situation could change the grid voltage significantly as the rated power of

the motor is large. The WT behavior could be affected because the asynchronous machine is very sensitive to the grid voltage. Again, the proposed controllers manage to make the WT behave in a very smooth way despite the large disturbance. In Figure 11a the motor speed is shown and the grid voltage is shown in Figure 11b. The output of the WP is shown in Figure 11c.

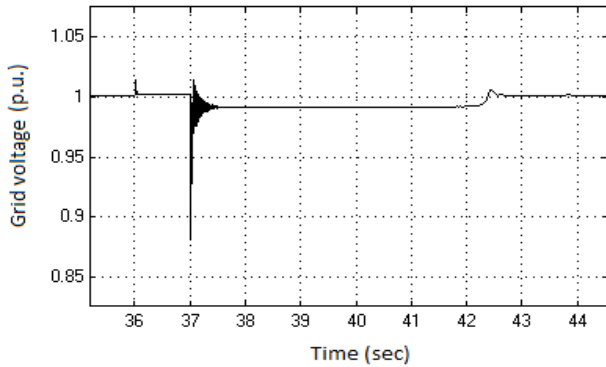


Figure 11b. Grid voltage under load disturbance

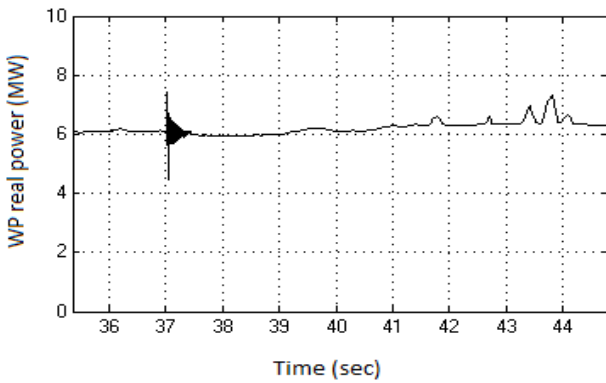


Figure 11c. WP real power for load disturbance

5. Conclusions

A control system that takes into account all the flux dynamics has been proposed for application to a wind turbine using an induction generator. The real decoupling between the real and the reactive power loops inside the machine have as a result an improved performance of the generator especially in transient state. The control systems were designed through optimal control theory with stochastic principles. The results of the nonlinear system are very good under vast changes of the wind speed, short-circuit state and load disturbances. The cooperation of the controllers ensure that the voltage and the frequency are within acceptable limits.

References

- [1] Custem, T.V., and Vournas, C.D. (1998). *Voltage Stability of the Electric Power System*, Kluwer Academic, Norwell.
- [2] Berizzi A. *The Italian 2003 blackout*, IEEE power engineering society general meeting, Denver, CO, pp 1673-1679.
- [3] Wu Q, Xu Z, Ostergaard J. *Grid Integration Issues for Large Scale Wind Power Plants*, IEEE power and energy society general meeting, Minneapolis, Minnesota, pp 1-6.

- [4] Interconnection for Wind Energy, Tech. rep., Order No. 661, 70 Fed. Reg. 34993 (FERC Stats. & Regs. 31, 186 (2005).
- [5] Krause, P., and Wasynczuk, O. (2010). *Analysis of Electrical Machinery*, IEEE Press.
- [6] Jahangir H., and Hemanshu R.P. (2014). *Robust Control for Grid Voltage Stability: High Penetration of Renewable Energy*, Springer.
- [7] Abad, G., Lopez, J., Rodriguez, M.A., Marroyo, L., and Iwanski, G. (2011). *Doubly Fed Induction Machine*, IEEE Press.
- [8] Robert F.S. (1993). *Optimal Control and Estimation*, Dover, New York.
- [9] Astrom, K.J., and Wittenmark, B. (2013). *Computer Controlled Systems*, Dover, New York.
- [10] Kersaoui, M., Chaib, A., Bendaoui, B., and Achour, D. (2016). *Grid voltage local regulation by a doubly fed induction generator – based wind turbine*, Wind Engineering, 41(1), pp. 13-25.
- [11] Schinas, N., and Papazafeiropoulos, C. (2016). *State-feedback and observer – based control design of a hybrid system consisting of a steam power plant in cooperation with a doubly fed wind turbine*, Wind Engineering, 40(3), pp. 199-211.

Appendix

Table A1. WT PARAMETERS [5,6]

Low speed inertia H_l	800 kgm ²
Coupling stiffness K_s	12500 Nm/rad
High speed inertia H_g	90 kgm ²
Nominal active power P_N	2 MW
Nominal electrical torque T_{elN} or T_g	9555 Nm
Stator voltage V_{SN}	575 V
Nominal generator speed n_{g0}	1800 rpm
Speed range of generator	900-1850 rpm
Pole pairs	2
Blades diameter d	80 m
Nominal wind speed V_{wN}	11.4 m/sec
Maximum power coefficient C_p	0.44
Air density	1.125 kg/m ³
Nominal turbine speed n_{t0}	22.5 rpm
Speed range of turbine speed	9-23 rpm
TSR optimum	8.7
Rotor resistance R_r	0.0011Ω
Rotor inductance	2.8 mH
Mutual inductance	3 mH
Stator inductance	3.12 mH
Stator voltage operating point	$V_{ds0} = 563.4$ V, $V_{qs0} = 0$ V
Rotor magnetic flux operating point (wb)	$\lambda_{dr0} = 0.4$ $\lambda_{qr0} = -1.86$
Rotor voltage operating point (V)	$V_{dr0} = -114.7$ $V_{qr0} = -25.8$
Rotor current operating point (A)	$I_{dr0} = 1846$ $I_{qr0} = -600$
Grid side components	$R_g = 0.33$ mΩ $L_g = 0.032$ H
Grid side current operating point (A)	$I_{dg} = -510$ $I_{qg} = -7$
Grid side voltage operating point (V)	$V_{dg} = 563.18$ $V_{qg} = 16$

Table A2. MEDIUM VOLTAGE LINE

Rated voltage V_N	25 kV
Inductive reactance X_o	2.917 Ω/km
Total Length	20 km

Table A3. ASYNCHRONOUS MOTOR PARAMETERS

Nominal power S_N	1.6 MVA
Nominal stator voltage V_{SN}	3.2 kV
Nominal frequency f	50 Hz
Inertia coefficient H	0.5 sec
Friction factor F	0.01 p.u.
Pole pairs	2